Remote-controlled exchange rates by photoswitchable internal catalysis of dynamic covalent bonds

David N. Barsoum, Viraj C. Kirinda,† Boyeong Kang,† Julia A. Kalow*

Department of Chemistry, Northwestern University, Evanston, Illinois 60208, United States

Photoswitch, dynamic covalent chemistry, boronic ester, internal catalysis

ABSTRACT: The transesterification of boronate esters with diols is tunable over 14 orders of magnitude. Rate acceleration is achieved by internal base catalysis, which lowers the barrier for proton transfer. Here we report a photoswitchable internal catalyst that tunes the rate of boronic ester/diol exchange over 4 orders of magnitude. We employed an acylhydrazone molecular photoswitch, which forms a thermally stable but photoreversible intramolecular H-bond, to gate the activity of the internal base catalyst in 8-quinoline boronic ester. The photoswitch is bidirectional and can be cycled repeatedly. The intramolecular H-bond is found to be essential to the design of this photoswitchable internal catalyst, as protonating the quinoline with external sources of acid has little effect on the exchange rate.

Dynamic covalent chemistry (DCC) combines the strength and directionality of covalent bonds with the reversibility of supramolecular interactions.[1] Owing to their tunability and robustness, dynamic covalent bonds have found wide application in library synthesis,[2] bioconjugation,[3] self-assembled macrocycles and cages,[4] covalent organic frameworks,[5] and self-healing polymers.[6] Light is an attractive stimulus to modulate the formation and exchange of these bonds because it can be applied non-invasively with excellent spatial and temporal control. Photoswitches, which can be reversibly switched between two states using different wavelengths of light, offer a unique opportunity to remotely control DCC.[7]

Previously, photoswitches have been employed to govern the reactivity of dynamic covalent bonds via two principal strategies: (i) by rendering the dynamic bond active or inactive through light-driven valence bond tautomerization;[8–10] and (ii) by tuning the reactivity of the dynamic bond with an adjacent photoswitch.[11–14] Hecht used azobenzene and spiropyran photoswitches to mask/unmask an activating hydroxyl group *ortho* to an aldehyde, which tunes the kinetics of imine formation by 2.4- and 3.1-fold, respectively.[15] Our group recently showed that azobenzene photoswitches can control the equilibrium of the boronic acid–diol condensation, due in part to the formation of intramolecular H-bonds (Figure 1A).[16] This change in thermodynamics was translated into hydrogels with reversibly photocontrolled stiffness.[17] However, the azobenzene boronic ester design was not effective for photocontrolling *kinetics*, displaying only 2.5-fold change in transesterification rate upon photoisomerization (see Supporting Information (SI), Figure S6).

Here, we present a strategy to remotely control the kinetics of dynamic covalent reactions by designing a photoswitch that modulates the reactivity of an internal catalyst. We have termed this approach photoswitchable internal catalysis (PIC). This is distinct from photoswitchable "external" catalysis, in which exogenous photoswitchable catalysts are introduced to modulate a structurally separate exchange reaction.[18,19] Internal catalysis, in contrast, exploits proximity effects (neighboring-group participation) to alter the kinetics of a dynamic covalent reaction.[20–24] While internal catalysis involves a 1:1 molar ratio of the neighboring group and dynamic covalent bond, the group can be considered catalytic because multiple exchanges (turnovers) occur at the dynamic covalent site without its consumption.[25] PIC can be applied to associative, degenerate exchange, whereas valence bond tautomerization has only been demonstrated for dissociative reactions such as Diels–Alder cycloaddition.

We report a PIC design that is capable of switching the exchange rate between boronic ester and free diol over 4 orders of magnitude (Figure 1B). Boronic ester transesterification represents an ideal chemistry to demonstrate PIC due to its wide dynamic range. In 1984, Wulff reported that the rate of exchange of boronic ester with diols spans a remarkable 14 orders of magnitude depending on the structure.[26] Wulff proposed that the exchange reaction proceeds via three fundamental steps: (I) addition, (II) proton transfer, and (III) elimination (Figure 1C). Small changes in structure can alter the identity of the rate-limiting step, resulting in a dramatic change in rates (Figure 2B). In simple phenylboronic esters, proton transfer was determined to be rate limiting (II>III>I). B–N coordination or steric hindrance slow the exchange by increasing the barrier for addition (I>II>III). In contrast, installing a proximal basic group significantly decreases the barrier for proton transfer through internal catalysis, making elimination rate limiting (III>II>I). While the commonly used 2-aminomethyl "Wulff-type" phenylboronic esters exhibit this effect, the rate enhancement is even greater in **8-QBE**, thanks to the proximity of the quinoline nitrogen lone pair to the boronic ester[27,28] and the rigid aromatic structure.[29]

We imagined that the rate-limiting step of boronic ester exchange could be remotely tuned with an appropriate photoswitch, thus altering the rate of exchange. Our strategy was to deactivate internal catalysis in **8-QBE** by engaging the quinoline lone pair in an intramolecular H-bond. Our attention was drawn to a class of

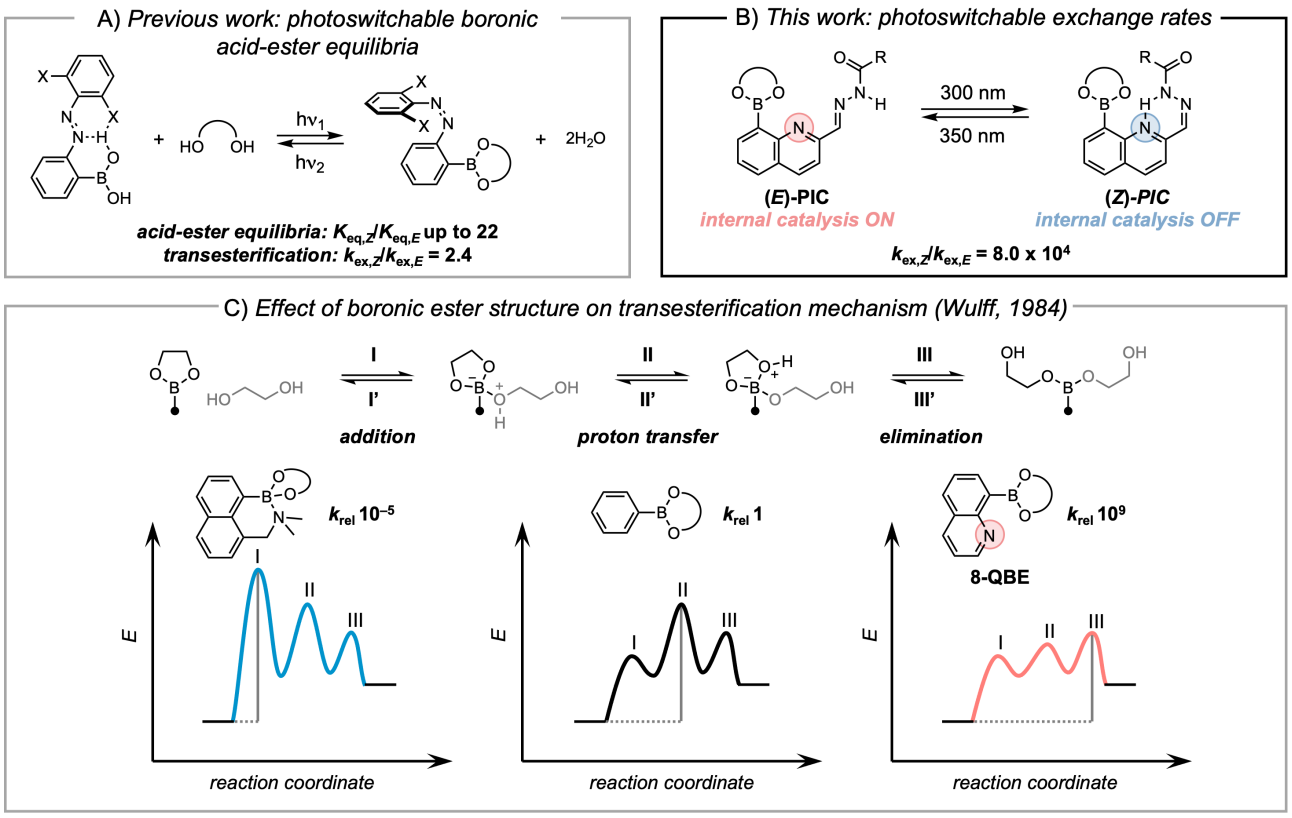

Figure 1. A) We previously showed that the conformation of an azobenzene influences the binding constant of a proximal boronic acid–diol dynamic bond, but there is little effect on the rate of transesterification. B) In this work, we design a hydrazone photoswitch that gates the activity of an internal catalyst (highlighted) to control the rate of transesterification. C) Mechanism of degenerate exchange of boronate ester and free diol. The forward reactions (I→II→III) are followed by identical reverse steps (III' → II' → I') to generate the final product. Corresponding reaction coordinate diagrams show the change in rate-limiting step depending on the boronic ester structure and rates relative to phenylboronic ester. For simplicity, the reaction coordinate diagram shows only I→II→III.

acylhydrazone photoswitches that bear an acidic amide N–H bond.[30–33] Acylhydrazones derived from 2-pyridinecarboxyaldehyde or 2-quinolinecarboxaldehyde are thermally stable in the *Z* isomer thanks to the formation of a six-membered intramolecular H-bond.[34] We envisioned that the intramolecular H-bond, in addition to stabilizing the *Z*-isomer, could deactivate internal catalysis in **8-QBE**. This design yielded **PIC** (Figure 1B), wherein exchange is accelerated by internal catalysis when the hydrazone adopts the *E* configuration and slowed in the *Z* isomer.

We synthesized the boronic acid **(*E*)-PIC$_{acid}$** in 6 steps from 2-bromoaniline and crotonaldehyde (see SI for details). First, we investigated its photoisomerization by monitoring the conversion from *E* to *Z* by ^{1}H NMR in DMSO-d_6. Initially, a sharp singlet appears at 12.23 ppm in the *E* isomer, corresponding to the free acylhydrazone N–H bond, and at 9.47 ppm, corresponding to the H-bonded boronic acid (Figure 2A and S25). Irradiation at 300 nm promotes conversion from **(*E*)-PIC$_{acid}$**→**(*Z*)-PIC$_{acid}$** (Figure 2B). After isomerization, the N–H peak shifts downfield to 14.33 ppm, indicating the formation of a strong intramolecular H-bond, and the O–H peak shifts upfield to 8.37 ppm. In the boronic acid form, the *Z* isomer is relatively unstable, with a thermal half-life of 7.3 hours at 25 °C (Figure S2). This relatively short half-life is ascribed to the acidity of the boronic acid, which accelerates thermal isomerization.[35] *Z*→*E* isomerization is promoted by 350 nm irradiation. After condensation with excess neopentyl glycol, bidirectional switching between **(*E*)-** and **(*Z*)-PIC$_{ester}$** with 300 (93% *Z* PSS) and 350 (56% *E* PSS) nm light is observed in DMSO-d_6 (Figure S3). Furthermore, **(*Z*)-PIC$_{ester}$** displays significantly improved thermal stability, with an extrapolated thermal half-life of 102 days at 25 °C (Figure S2). We anticipate that derivatization of the acylhydrazone will enable further optimization of the photochemical properties.[33]

The fatigue resistance of other hydrazone photoswitches is quite high (up to 300 cycles).[33,36] Using UV-Vis, we monitored *E*→*Z* isomerization of **PIC$_{acid}$** over time during irradiation at 300 and 350 nm and found that the *Z* and *E* PSS are reached within 1 and 2 minutes, respectively, in acetonitrile at 1.56×10^{-5} M (Figure S5). Monitoring the UV-Vis absorption of **PIC$_{acid}$** at 322 nm during alternating irradiation at 300 and 350 nm, we observe no loss in efficiency after 10 cycles under ambient conditions (Figure 2C). Therefore, the presence of a boronic acid does not affect the robustness of the hydrazone photoswitch.

We tested the effect of photoisomerization on the degenerate exchange between neopentyl glycol and the corresponding boronic

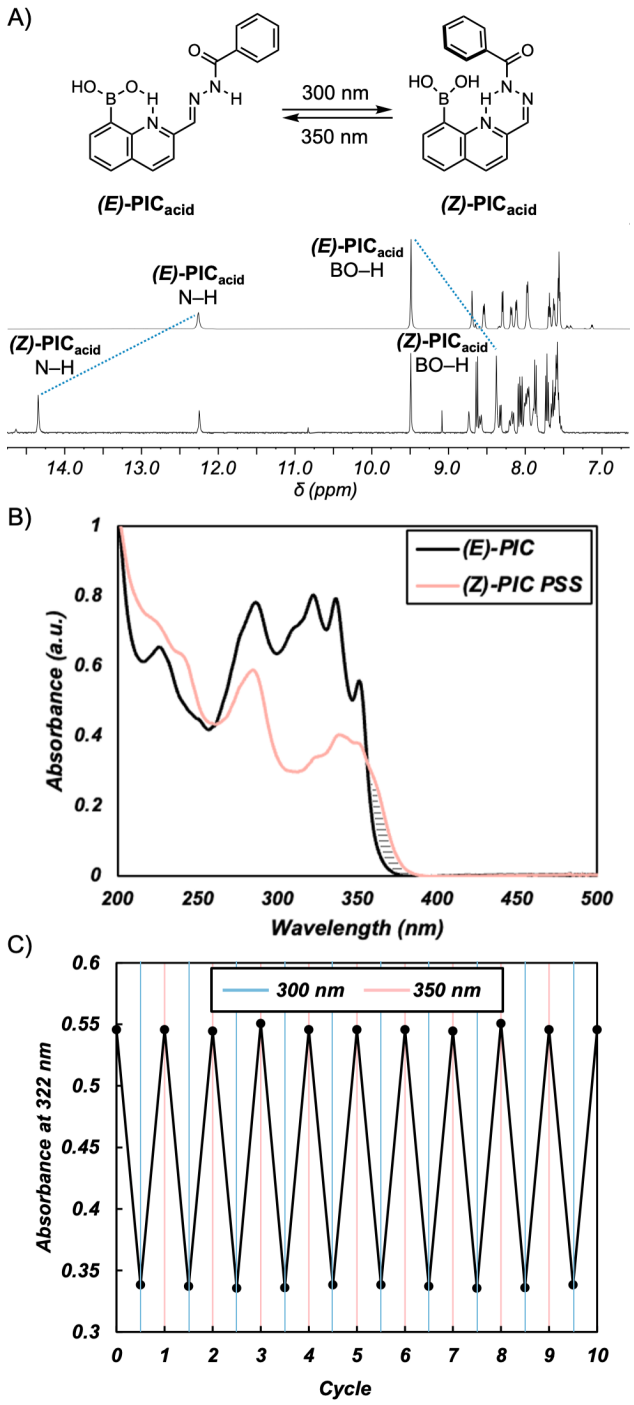

Figure 2. A) ^{1}H NMR of the aromatic region of **(*E*)-** and **(*Z*)-PIC$_{acid}$** shows the N–H and BO–H peak shifts after isomerization in DMSO-d_6. B) UV-Vis absorbance of **(*E*)-PIC$_{acid}$** (black line) and the photostationary state of **(*Z*)-PIC$_{acid}$** (red line) (acetonitrile, 1.56×10^{-5} M). C) Absorbance of **PIC$_{acid}$** at 322 nm during cycles of irradiation at 300 nm (blue lines) and 350 nm (red lines).

ester **(*E*)-PIC$_{ester}$** (1:1, 100 mM). Toluene was used as the solvent, and a small amount of acetone was added to fully dissolve the diol (9:1 toluene-acetone). At 25 °C, ^{1}H NMR of **(*E*)-PIC$_{ester}$** shows a broad peak around 1.0 ppm, signifying that the dynamic exchange between diol and ester is occurring faster than the NMR timescale at this temperature. The rate of exchange in **(*E*)-PIC$_{ester}$** could be determined through coalescence between $-CH_3$ resonances in bound and unbound neopentyl glycol by variable-temperature ^{1}H NMR (VT-NMR). Upon cooling the mixture, we observe the coalescence temperature of the bimolecular degenerate exchange to be -15 ± 5 °C (Figure 3). The rate of exchange for **(*E*)-PIC$_{ester}$** was thus determined to be $4.1 \pm 1.4 \times 10^3$ s^{-1} at 25 °C with an activation energy of 12.4 ± 0.2 kcal/mol (see SI for details). A second coalescence temperature is observed at lower temperatures due to a unimolecular fluxional ring flip of the neopentylglycol boronate (Figure S8).[37]

After irradiation with 300 nm light to form **(*Z*)-PIC$_{ester}$**, the bimolecular exchange is significantly slowed, and a coalescence temperature could not be observed even at elevated temperatures (Figure S10). Therefore, we monitored the transesterification using ^{1}H–^{1}H 2D exchange spectroscopy (EXSY) NMR at 45 °C, revealing an exchange rate of 0.19 ± 0.01 s^{-1} (Figure 3). Using the VT-NMR data, we calculate that the exchange rate for **(*E*)-PIC$_{ester}$** at 45 °C is 1.5×10^4 s^{-1}. Therefore, the relative rate of exchange $k_{ex,E}/k_{ex,E}$ is 8.0×10^4. This k_{rel} value is 3–4 orders of magnitude larger than those achieved by previous photoswitch designs[15,17,38] and suggests the potential for PIC as a strategy to remotely control the rates of associative exchange reactions. In addition to PIC, it is possible that the effect of photoswitch conformation on the Lewis acidity of the boronic ester contributes to rate differences.[39] The effect of the photoswitch was qualitatively observed for other diols (pinacol, 1,2-propanediol) but k_{rel} could not be measured for both isomers (Figures S20-21). Exchange is slowed in more polar solvents such as DMF-d_7, but a significant difference in *E* and *Z* exchange rates is maintained (Figures S16-S19).

To show that chemical stimuli cannot regulate internal catalysis to the same extent, we synthesized the neopentyl glycol ester of (2-methylquinolin-8-yl)boronic acid (**Me-QBE**, SI). VT-NMR revealed that **Me-QBE** undergoes exchange roughly 10 times faster than to **(*E*)-PIC$_{ester}$** (~4.9×10^4 s^{-1} at 25 °C, Figure S6). We hypothesize that the electron-withdrawing hydrazone in **(*E*)-PIC$_{ester}$** reduces the basicity of the quinoline, slowing exchange relative to **Me-QBE**. When **Me-QBE** is exposed to 1.0 equivalent of trifluoroacetic acid (TFA), an acid capable of fully protonating the quinoline, only a moderate decrease in exchange rates was observed (~3.0×10^4 s^{-1} at 25 °C, Figure S7). This observation is consistent with the fact that esterification of boronic acids can be catalyzed by both acid and base,[40,41] so external proton sources cannot deactivate internal catalysis. These experiments further highlight the importance the intramolecular H-bond in our design to deactivate internal catalysis. Additionally, Letsinger[27] and Wulff[26] have shown that the presence of exogeneous quinoline does not increase the transesterification rate for simple phenylboronic esters, indicating that the high effective molarity provided by internal catalysis is crucial for accelerating exchange.

Guan has shown that internal catalysis of boronic ester[20] and silyl ether[21] exchange provides five and three orders of magnitude rate acceleration, respectively. These differences in small-molecule exchange rates were translated into significant and measurable differences in the physical properties of polymer networks (self-healing ability and stress relaxation), suggesting that the observed k_{rel} of 8.0×10^4 is sufficient to mediate macroscopic changes. We

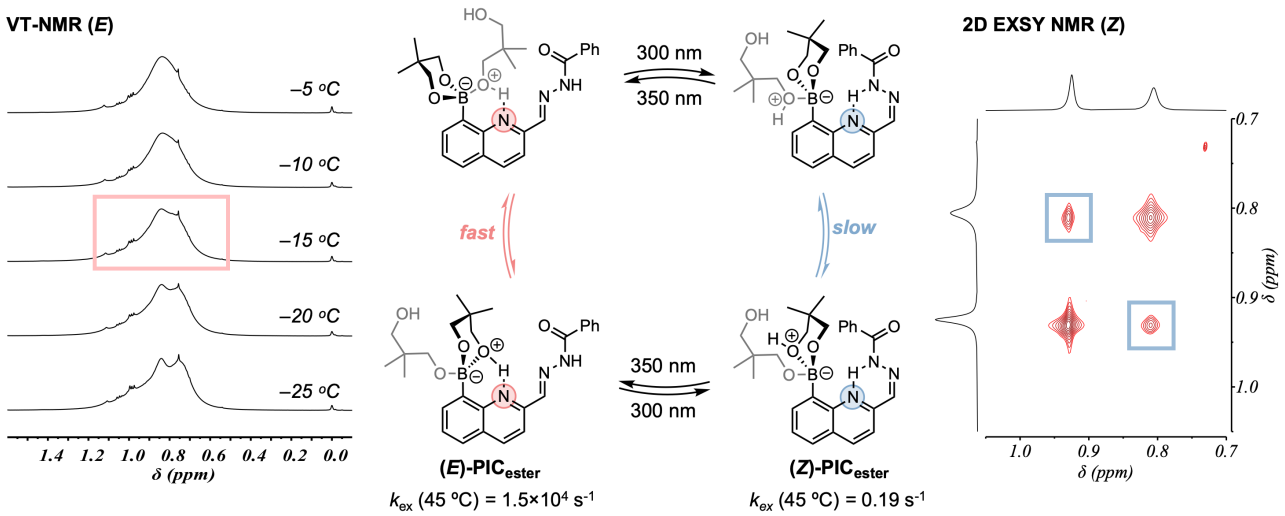

Figure 3. ^{1}H VT-NMR of the diol–ester exchange of **(*E*)-PIC$_{ester}$** (left, T_c highlighted) and ^{1}H–^{1}H 2D EXSY NMR of the exchange of **(*Z*)-PIC$_{ester}$** (right, crosspeaks highlighted) (1:1 diol:ester, 0.1 M in 9:1 toluene-d$_8$-acetone). The proposed effect of the photoswitch on the proton transfer step is illustrated in the center.

prepared a viscoelastic polymer network by condensation of 4-arm poly(caprolactone) with **(*E*)-PIC$_{acid}$** at elevated temperature.[42–44] Using oscillatory shear rheology at 100 °C, we observed a decrease in the crossover frequency corresponding to slower exchange kinetics when the network was photoswitched at 300 nm (Figures S23-24). No change in storage modulus was observed, consistent with an associative mechanism.[6]

We have demonstrated the use of a bidirectional hydrazone photoswitch to control the rate of exchange between boronate ester and diol over 4 orders of magnitude. The dramatic change in rates afforded by reversible deactivation of internal catalysis lays the foundation for photocontrolling kinetics in different dynamic covalent reactions. The ability to remotely and reversibly control a dynamic covalent exchange rate can be translated to turn on and off assembly and reconfiguration in smart materials. The design of photoswitchable internal catalysts for dynamic reactions that can be incorporated into photocontrolled hydrogels is ongoing in our laboratory.[45]

ASSOCIATED CONTENT

Supporting Information. Synthetic procedures; NMR data; photochemical characterization; additional experiments.

AUTHOR INFORMATION

Corresponding Author

* jkalow@northwestern.edu

Author Contributions

†These authors contributed equally.

ACKNOWLEDGMENT

This material is based upon work supported by the National Science Foundation under CAREER CHE-1847948. D.N.B. acknowledges support from a National Science Foundation Graduate Research Fellowship (grant no. DGE-1842165). J.A.K. is supported by a Sloan Research Fellowship, a Dreyfus Teacher-Scholar Award, and a 3M Non-Tenured Faculty Award. This work made use of NMR and MS instrumentation at the Integrated Molecular Structure Education and Research Center (IMSERC) at Northwestern, which has received support from the NSF (NSF CHE-9871268); Soft and Hybrid Nanotechnology Experimental (SHyNE) Resource (NSF ECCS-1542205); the State of Illinois and International Institute for Nanotechnology. Rheological measurements were performed at the MatCI Facility, which receives support from the MRSEC Program (NSF DMR-1720139) of the Materials Research Center at Northwestern University. Jonathan Sklar is acknowledged for assistance with the analysis of X-ray crystallographic data.

REFERENCES

(1) Rowan, S. J.; Cantrill, S. J.; Cousins, G. R. L.; Sanders, J. K. M.; Stoddart, J. F. Dynamic Covalent Chemistry. Angew. Chem. Int. Ed. 2002, 41 (6), 898–952. https://doi.org/10.1002/1521-3773(20020315)41:6<898::AID-ANIE898>3.0.CO;2-E.

(2) Li, J.; Nowak, P.; Otto, S. Dynamic Combinatorial Libraries: From Exploring Molecular Recognition to Systems Chemistry. J. Am. Chem. Soc. 2013, 135 (25), 9222–9239. https://doi.org/10.1021/ja402586c.

(3) Ulrich, S. Growing Prospects of Dynamic Covalent Chemistry in Delivery Applications. Acc. Chem. Res. 2019, 52 (2), 510–519. https://doi.org/10.1021/acs.accounts.8b00591.

(4) Jin, Y.; Wang, Q.; Taynton, P.; Zhang, W. Dynamic Covalent Chemistry Approaches Toward Macrocycles, Molecular Cages, and Polymers. Acc. Chem. Res. 2014, 47 (5), 1575–1586. https://doi.org/10.1021/ar500037v.

(5) Evans, A. M.; Strauss, M. J.; Corcos, A. R.; Hirani, Z.; Ji, W.; Hamachi, L. S.; Aguilar-Enriquez, X.; Chavez, A. D.; Smith, B. J.; Dichtel, W. R. Two-Dimensional Polymers and Polymerizations. Chem. Rev. 2022, 122 (1), 442–564. https://doi.org/10.1021/acs.chemrev.0c01184.

(6) Winne, J. M.; Leibler, L.; Du Prez, F. E. Dynamic Covalent Chemistry in Polymer Networks: A Mechanistic Perspective. Polym. Chem. 2019, 10 (45), 6091–6108. https://doi.org/10.1039/C9PY01260E.

(7) Kathan, M.; Hecht, S. Photoswitchable Molecules as Key Ingredients to Drive Systems Away from the Global Thermodynamic Minimum. Chem. Soc. Rev. 2017, 46 (18), 5536–5550. https://doi.org/10.1039/c7cs00112f.

(8) Lemieux, V.; Gauthier, S.; Branda, N. R. Selective and Sequential Photorelease Using Molecular Switches. Angew. Chem. Int. Ed. 2006, 118 (41), 6974–6978. https://doi.org/10.1002/ange.200601584.

(9) Göstl, R.; Hecht, S. Controlling Covalent Connection and Disconnection with Light. Angew. Chem. Int. Ed. 2014, 53 (33), 8784–8787. https://doi.org/10.1002/anie.201310626.

(10) Kathan, M.; Eisenreich, F.; Jurissek, C.; Dallmann, A.; Gurke, J.; Hecht, S. Light-Driven Molecular Trap Enables Bidirectional Manipulation of Dynamic Covalent Systems. Nature Chem. 2018, 10 (10), 1031–1036. https://doi.org/10.1038/s41557-018-0106-8.

(11) Kano, N.; Komatsu, F.; Kawashima, T. Reversible Photocontrol of the Coordination Number of Silicon in a Tetrafluorosilicate Bearing a 2-(Phenylazo)Phenyl Group. J. Am. Chem. Soc. 2001, 123 (43), 10778–10779. https://doi.org/10.1021/ja0165739.

(12) Kano, N.; Yamamura, M.; Kawashima, T. Reactivity Control of an Allylsilane Bearing a 2-(Phenylazo)Phenyl Group by Photoswitching of the Coordination Number of Silicon. J. Am. Chem. Soc. 2004, 126 (20), 6250–6251. https://doi.org/10.1021/ja037404m.

(13) Kano, N.; Yoshino, J.; Kawashima, T. Photoswitching of the Lewis Acidity of a Catecholborane Bearing an Azo Group Based on the Change in Coordination Number of Boron. Org. Lett. 2005, 7 (18), 3909–3911. https://doi.org/10.1021/ol051337e.

(14) Yoshino, J.; Kano, N.; Kawashima, T. Synthesis of Organoboron Compounds Bearing an Azo Group and Substituent Effects on Their Structures and Photoisomerization. Tetrahedron 2008, 64 (33), 7774–7781. https://doi.org/10.1016/j.tet.2008.05.128.

(15) Kathan, M.; Kovaříček, P.; Jurissek, C.; Senf, A.; Dallmann, A.; Thünemann, A. F.; Hecht, S. Control of Imine Exchange Kinetics with Photoswitches to Modulate Self-Healing in Polysiloxane Networks by Light Illumination. Angew. Chem. Int. Ed. 2016, 55 (44), 13882–13886. https://doi.org/10.1002/anie.201605311.

(16) Accardo, J. V.; McClure, E. R.; Mosquera, M. A.; Kalow, J. A. Using Visible Light to Tune Boronic Acid-Ester Equilibria. J. Am. Chem. Soc. 2020, 142 (47), 19969–19979. https://doi.org/10.1021/jacs.0c08551.

(17) Accardo, J. V.; Kalow, J. A. Reversibly Tuning Hydrogel Stiffness through Photocontrolled Dynamic Covalent Crosslinks. Chem. Sci. 2018, 9 (27), 5987–5993. https://doi.org/10.1039/C8SC02093K.

(18) Neilson, B. M.; Bielawski, C. W. Illuminating Photoswitchable Catalysis. ACS Catal. 2013, 3 (8), 1874–1885. https://doi.org/10.1021/cs4003673.

(19) Dorel, R.; Feringa, B. L. Photoswitchable Catalysis Based on the Isomerisation of Double Bonds. Chem. Commun. 2019, 55 (46), 6477–6486. https://doi.org/10.1039/c9cc01891c.

(20) Cromwell, O. R.; Chung, J.; Guan, Z. Malleable and Self-Healing Covalent Polymer Networks through Tunable Dynamic Boronic Ester Bonds. J. Am. Chem. Soc. 2015, 137 (20), 6492–6495. https://doi.org/10.1021/jacs.5b03551.

(21) Nishimura, Y.; Chung, J.; Muradyan, H.; Guan, Z. Silyl Ether as a Robust and Thermally Stable Dynamic Covalent Motif for Malleable Polymer Design. J. Am. Chem. Soc. 2017, 139 (42), 14881–14884. https://doi.org/10.1021/jacs.7b08826.

(22) Delahaye, M.; Winne, J. M.; Du Prez, F. E. Internal Catalysis in Covalent Adaptable Networks: Phthalate Monoester Transesterification As a Versatile Dynamic Cross-Linking Chemistry. J. Am. Chem. Soc. 2019, 141 (38), 15277–15287. https://doi.org/10.1021/jacs.9b07269.

(23) Van Lijsebetten, F.; Holloway, J. O.; Winne, J. M.; Du Prez, F. E. Internal Catalysis for Dynamic Covalent Chemistry Applications and Polymer Science. Chem. Soc. Rev. 2020, 49 (23), 8425–8438. https://doi.org/10.1039/d0cs00452a.

(24) Cuminet, F.; Caillol, S.; Dantras, E.; Leclerc, E.; Ladmiral, V. Neighboring Group Participation and Internal Catalysis Effects on Exchangeable Covalent Bonds: Application to the Thriving Field of Vitrimer Chemistry. Macromolecules 2021. https://doi.org/10.1021/acs.macromol.0c02706.

(25) Muller, P. Glossary of Terms Used in Physical Organic Chemistry (IUPAC Recommendations 1994). Pure and Applied Chemistry 1994, 66 (5), 1077–1184. https://doi.org/10.1351/pac199466051077.

(26) Wulff, G.; Lauer, M.; Böhnke, H. Rapid Proton Transfer as Cause of an Unusually Large Neighboring Group Effect. Angew. Chem. Int. Ed. Engl. 1984, 23 (9), 741–742. https://doi.org/10.1002/anie.198407411.

(27) Letsinger, R. L.; Dandegaonker, S. H. Organoboron Compounds. IX. 8-Quinolineboronic Acid, Its Preparation and Influence on Reactions of Chlorohydrins 1. J. Am. Chem. Soc. 1959, 81 (2), 498–501. https://doi.org/10.1021/ja01511a060.

(28) Morrison, J. D.; Letsinger, R. L. Organoboron Compounds. XVIII. Bifunctional Binding of Water by the Cis-1,2-Cyclopentanediol Ester of 8-Quinolineboronic Acid. J. Org. Chem. 1964, 29 (11), 3405–3407. https://doi.org/10.1021/jo01034a505.

(29) Goldman, M.; Wehry, E. L. Environmental Effects upon the Photoluminescence of 8-Quinolineboronic Acid. Anal. Chem. 1970, 42 (11), 1186–1188. https://doi.org/10.1021/ac60293a046.

(30) Chaur, M. N.; Collado, D.; Lehn, J. M. Configurational and Constitutional Information Storage: Multiple Dynamics in Systems Based on Pyridyl and Acyl Hydrazones. Chem. Eur. J. 2011, 17 (1), 248–258. https://doi.org/10.1002/chem.201002308.

(31) Su, X.; Aprahamian, I. Hydrazone-Based Switches, Metallo-Assemblies and Sensors. Chem. Soc. Rev. 2014, 43 (6), 1963–1981. https://doi.org/10.1039/c3cs60385g.

(32) Shao, B.; Aprahamian, I. Hydrazones as New Molecular Tools. Chem 2020, 6 (9), 2162–2173. https://doi.org/10.1016/j.chempr.2020.08.007.

(33) Van Dijken, D. J.; Kovaříček, P.; Ihrig, S. P.; Hecht, S. Acylhydrazones as Widely Tunable Photoswitches. J. Am. Chem. Soc. 2015, 137 (47), 14982–14991. https://doi.org/10.1021/jacs.5b09519.

(34) Romero, E. L.; D'Vries, R. F.; Zuluaga, F.; Chaur, M. N. Multiple Dynamics of Hydrazone Based Compounds. J. Braz. Chem. Soc. 2015, 26 (6), 1265–1273. https://doi.org/10.5935/0103-5053.20150092.

(35) Landge, S. M.; Tkatchouk, E.; Benítez, D.; Lanfranchi, D. A.; Elhabiri, M.; Goddard, W. A.; Aprahamian, I. Isomerization Mechanism in Hydrazone-Based Rotary Switches: Lateral Shift, Rotation, or Tautomerization? J. Am. Chem. Soc. 2011, 133 (25), 9812–9823. https://doi.org/10.1021/ja200699v.

(36) Qian, H.; Pramanik, S.; Aprahamian, I. Photochromic Hydrazone Switches with Extremely Long Thermal Half-Lives. J. Am. Chem. Soc. 2017, 139 (27), 9140–9143. https://doi.org/10.1021/jacs.7b04993.

(37) Eichhorn, A. Copper(I) Catalyzed Borylation and Cross-Coupling Reactions. PhD Thesis, Julius Maximilian University of Würzburg, Würzburg, Germany, 2018.

(38) De Bo, G.; Leigh, D. A.; McTernan, C. T.; Wang, S. A Complementary Pair of Enantioselective Switchable Organocatalysts. Chem. Sci. 2017, 8 (10), 7077–7081. https://doi.org/10.1039/c7sc02462b.

(39) Suzuki, Y.; Kusuyama, D.; Sugaya, T.; Iwatsuki, S.; Inamo, M.; Takagi, H. D.; Ishihara, K. Reactivity of Boronic Acids toward Catechols in Aqueous Solution. J. Org. Chem. 2020, 85 (8), 5255–5264. https://doi.org/10.1021/acs.joc.9b03326.

(40) Collins, B. E.; Metola, P.; Anslyn, E. V. On the Rate of Boronate Ester Formation in Ortho-Aminomethyl-Functionalised Phenyl Boronic Acids. Supramol. Chem. 2013, 25 (2), 79–86. https://doi.org/10.1080/10610278.2012.740044.

(41) Sun, X.; Chapin, B. M.; Metola, P.; Collins, B.; Wang, B.; James, T. D.; Anslyn, E. V. The Mechanisms of Boronate Ester Formation and Fluorescent Turn-on in Ortho-Aminomethylphenylboronic Acids. Nature Chem. 2019, 11 (9), 768–778. https://doi.org/10.1038/s41557-019-0314-x.

(42) Jing, B. B.; Evans, C. M. Catalyst-Free Dynamic Networks for Recyclable, Self-Healing Solid Polymer Electrolytes. J. Am. Chem. Soc. 2019, 141 (48), 18932–18937. https://doi.org/10.1021/jacs.9b09811.

(43) Soman, B.; Evans, C. M. Effect of Precise Linker Length, Bond Density, and Broad Temperature Window on the Rheological Properties of Ethylene Vitrimers. Soft Matter 2021, 17 (13), 3569–3577. https://doi.org/10.1039/D0SM01544J.

(44) Lv, G.; Soman, B.; Shan, N.; Evans, C. M.; Cahill, D. G. Effect of Linker Length and Temperature on the Thermal Conductivity of Ethylene Dynamic Networks. ACS Macro Lett. 2021, 10 (9), 1088–1093. https://doi.org/10.1021/acsmacrolett.1c00423.

(45) Kang, B.; Kalow, J. A. Internal and External Catalysis in Boronic Ester Networks. ACS Macro Lett. 2022, 11 (3), 394–401. https://doi.org/10.1021/acsmacrolett.2c00056.

TOC graphic:

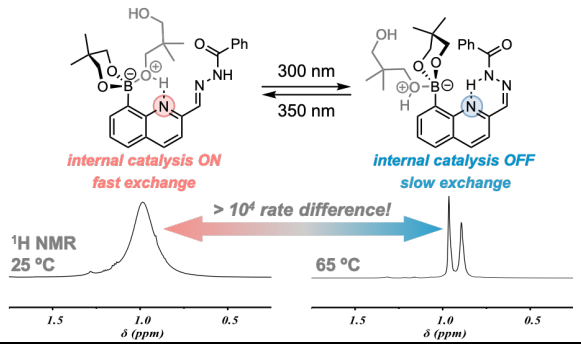
HO
Ph
O
NH
N
300 nm
350 nm
OH
internal catalysis ON
fast exchange
internal catalysis OFF
slow exchange
> 10⁴ rate difference!
¹H NMR
25 °C
65 °C
1.5
1.0
0.5
δ (ppm)